The Journal of Immunology

NF-{kappa}B Signaling, Elastase Localization, and Phagocytosis Differ in HIV-1 Permissive and Nonpermissive U937 Clones

Cynthia L. Bristow, Roland Wolkowicz, Maylis Trucy, Aaron Franklin, Fernando Di Meo, Mark T. Kozlowski, Ronald Winston and Roland R. Arnold

J. Immunol. 2008;180;492-499
http://www.jimmunol.org/cgi/content/full/180/1/492

The Journal of Immunology is published twice each month by The American Association of Immunologists, Inc., 9650 Rockville Pike, Bethesda, MD 20814-3994.

Print ISSN: 0022-1767 Online ISSN: 1550-6606.

NF-κB Signaling, Elastase Localization, and Phagocytosis Differ in HIV-1 Permissive and Nonpermissive U937 Clones[1]

Cynthia L. Bristow,[2]*† Roland Wolkowicz,‡ Maylis Trucy,* Aaron Franklin,* Fernando Di Meo,§ Mark T. Kozlowski,¶ Ronald Winston,* and Roland R. Arnold§

To identify positive or negative factors for HIV-1 infectivity, clones from the U937 promonocytic cell line that express similar levels of CD4 and CXCR4, but differ in HIV-1 susceptibility, were compared. In contrast to HIV-1 permissive clone 10 (plus), nonpermissive clone 17 (minus) was adherent to coverslips coated with chemokines, was phagocytic, killed bacteria, and expressed human leukocyte elastase (HLE) in a granule-like compartment (HLE_G) that was never detected at the cell surface (HLE_{CS}). In contrast to the minus clone, the plus clone expressed HLE on the cell surface and was adherent to coverslips coated with the HLE_{CS} ligands $\alpha_1$proteinase inhibitor (α_1PI, $\alpha_1$antitrypsin) and the HIV-1 fusion peptide. The phosphorylation status of several important signaling proteins was studied at the single cell level. Tumor suppressor p53, NF-κB p65, and Akt were constitutively phosphorylated in the plus clone, but not in the minus clone. Surprisingly, both α_1PI and LPS induced phosphorylation of NF-κB p65 Ser-536 in both clones, but induced dephosphorylation of Ser-529 in the plus clone only. HIV-1 permissivity was conferred to the minus clone in a manner that required stimulation by both α_1PI and LPS and was coincident to NF-κB p65 phosphorylation/dephosphorylation events as well as translocation of HLE to the cell surface. Even when stimulated, the minus clone exhibited greater reverse transcriptase activity, but less p24, than the plus clone. Results presented suggest that HIV-1 uptake and production efficiency are influenced by signaling profiles, receptor distribution, and the phagocytic capacity specific to the stage of differentiation of the $CD4^+$ target cell. ***The Journal of Immunology,*** **2008, 180: 492–499.**

The U937 cell line and its subclones (clone 10 and clone 17) represent dedifferentiated promonocytic cells which are genomically indistinguishable, yet they differ in gene expression and capacity to productively support HIV-1 infection. HIV-1 permissive (plus) and nonpermissive (minus) clones have been shown to express relatively equivalent levels of CD4 and CXCR4, do not express CCR5, and differ in the subcellular localization of human leukocyte elastase (HLE)[3] (1, 2). cell-surface HLE (HLE_{CS}) localizes exclusively to the cell surface of the plus clone, where it behaves as a receptor, and when bound to a ligand such as α_1PI, HLE_{CS}, clusters and cocaps with CD4 and CXCR4 in a plasma membrane configuration, which is rate limiting for HIV-1 binding and entry (2, 3). In contrast, granule-associated human leukocyte elastase (HLE_G) localizes exclusively to granules in the minus clone where it behaves as a species-specific proteinase that degrades a wide variety of substrates, including the chemokine stromal-derived factor 1 (SDF 1, CXCL12) and its cognate receptor CXCR4, and NF-κB (4). HLE_G and HLE_{CS} are synthesized and processed as a single molecular protein targeted for secretion early in ontogeny and for granule compartmentalization after granule formation is enabled (5). The differences in HLE localization suggest that U937 plus and minus clones have become arrested at disparate stages of maturation.

HLE_G and cathepsin G (CatG) are microbicidal components of azurophil granules, a subset of lysosome-related organelles. Microbe-interactive molecules are packaged within these vesicles, often in an inactive form. Traffic of these vesicles to the phagolysosome promotes vesicle fusion, granule mixing, proteinase activation, and liberation of a potent milieu of microbicidal peptides and reactive oxygen intermediates into a contained environment. Under pathologic conditions, soluble vesicle components are released to the extracellular environment.

In contrast, HLE_{CS} participates in cell mobility, transendothelial migration, and hematopoiesis (6, 7). Progenitor cell migration is a function of time and space and is mediated by CXCL12, CXCR4, and HLE_{CS}. Our current model of progenitor cell migration infers that cells are directionally regulated by the binding of CXCL12 to CXCR4 colocalized with HLE_{CS} at the leading edge of the migrating cell (7). It has been shown that at a fixed time point, coclustering of CXCR4 and HLE_{CS} is facilitated by the HLE ligand α_1PI and suppressed by CXCL12 (7), suggesting that the order of

*Institute for Human Genetics and Biochemistry and †Department of Medicine, Mount Sinai School of Medicine, New York, NY 10003; ‡Department of Biology, San Diego State University, San Diego, CA 92182; §Dental Research Center, University of North Carolina, Chapel Hill, NC 27599; and ¶Antara BioSciences, Mountain View, CA 94043

Received for publication June 29, 2007. Accepted for publication October 24, 2007.

The costs of publication of this article were defrayed in part by the payment of page charges. This article must therefore be hereby marked *advertisement* in accordance with 18 U.S.C. Section 1734 solely to indicate this fact.

[1] This work was supported by the University of North Carolina Center for AIDS Research and Harry Winston Research Foundation.

[2] Address correspondence and reprint requests to Dr. C. L. Bristow, Director of Research, Institute for Human Genetics and Biochemistry, Department of Medicine, Mount Sinai School of Medicine, 227 East 19th Street, Room D477, New York, NY 10003. E-mail address: Cynthia.Bristow@mssm.edu

[3] Abbreviations used in this paper: HLE, human leukocyte elastase; HLE_G, granule-associated HLE; HLE_{CS}, cell-surface HLE; TEM, transmission electron microscopy; DAPI, 4′-6-diamidino-2-phenylindole; PI, propidium iodide; α_1ACT α_1, antichymotrypsin; ATIII, antithrombin III; MAAPVCK, methoxysuccinyl-L-Ala-L-Ala-L-Pro-L-Val-chloromethylketone; TPCK, N-tosyl-L-phenylalanine chloromethylketone; INR, internally normalized ratio; LRP, lipoprotein receptor-related protein; CatG, cathepsin G.

receptor engagement may alter cell migration by changing spatial and/or temporal parameters. Although soluble HLE_G has the capacity to degrade CXCR4 and CXCL12 (8), degradation by HLE_{CS} does not occur during cell migration (9).

Whereas the U937 minus clone exhibits no cell surface HLE, bacterial LPS can induce the release of granule components including HLE, and under these circumstances, HLE localizes to the cell surface where it confers HIV-1 permissivity in a manner that requires the presence of α_1PI (2). Importantly, the fact that the LPS-stimulated minus clone can become infected with HIV-1 suggests that the minus clone contains the full complement of signaling and activation steps, including NF-κB, necessary for HIV-1 infectivity.

Paradoxically, the plus clone exhibits intact NF-κB p65, whereas the minus clone exhibits a truncated form of NF-κB p65 caused by the catabolic activity of HLE_G, proteinase 3, or CatG (10). NF-κB p65 truncation is also found in other granule-containing HIV-1 nonpermissive or suboptimally-permissive cells such as THP1, HL60, primary monocytes, chronically infected U1 cells (10), and CEM T lymphoblastoid cells (11). Truncated NF-κB p65 binds DNA, but lacks transactivation activity, suggesting that direct or indirect interaction of NF-κB p65 with HLE_G, CatG, or proteinase 3 negatively regulates HIV-1 replication before integration (10).

Herein plus and minus U937 clones have been compared by cell signaling, protein array analysis, bacterial phagocytosis, HIV-1 infectivity, and subcellular localization of NF-κB, HLE, and CatG. Results demonstrate that α_1PI and LPS each induce dephosphorylation of NF-κB p65 Ser-529 and phosphorylation of NF-κB p65 Ser-536. Importantly, because of receptor and signaling differences, equivalent uptake of particles of HIV-1 by these different clones did not result in equivalent production of virus.

Materials and Methods

Cells and reagents

U937 subclones were provided by the Laboratory of Immunoregulation, National Institute of Allergy and Infectious Diseases, National Institutes of Health, and maintained using RPMI 1640 containing 10% FBS (BioWhittaker, Sigma-Aldrich, and Invitrogen Life Technologies). All sera were determined to have endotoxin levels <0.3 EU/ml. In all experiments described, cells were harvested during exponential growth and were >95% viable as determined by trypan blue exclusion.

The functionally active concentrations of two preparations of α_1PI (Cat. no. A6150, lot no. 82H9323, Cat. no. A9024, lot no. 115H9320, Sigma-Aldrich) were determined using active-site titrated porcine pancreatic elastase, type 1 (PPE, EC 3.4.21.36, Sigma) as previously described (12).

Immunocytochemical transmission electron microscopy (TEM)

TEM was performed by Wallace Ambrose, Microscopy Laboratory, Dental Research Center, University of North Carolina-Chapel Hill. Grids were etched and stained using rabbit anti-HLE (Biodesign), anti-CatG (Biodesign), or anti-NF-κB p50 (Biodesign) at concentrations of 1 mg/ml in 0.01 M phosphate, 0.15 M NaCl (pH 7.2; PBS). Ab binding was detected using Protein A polygold (0.23 μg/ml, Sigma-Aldrich) and photographed using a Philips CM/12 TEM/STEM transmission electron microscope. Negative control grids were stained without primary Ab.

Phagocytosis and bacterial killing of opsonized bacteria

Porphorymonas gingivalis Strain A7436 was harvested during exponential growth, pelleted, and resuspended in 1 ml saline. Bacteria were labeled with the dsDNA-binding fluorescent dye 4′-6-diamidino-2-phenylindole (DAPI), washed and resuspended at 2.0×10^8 CFU/ml. Propidium iodide (PI) is a DNA-binding fluorescent dye excluded by intact cell membranes and was added to the bacterial suspension. Phagocytosis of bacterial suspensions containing PI induces phagosomal localization of PI. Its red color quenches the blue color of DAPI allowing easily discernible viability of phagocytosed bacteria. Bacteria were opsonized using Ab (20% rabbit antiserum specific for *P. gingivalis*) and complement (20% human serum, type AB). Opsonized bacteria (2.0×10^7 CFU) were incubated with cells (4.0×10^5 cells) in HBSS containing 0.06 μM $CaCl_2$, 0.05 μM $MgCl_2$, and the nuclear staining fluorescent dye acridine orange (3,6-bis[dimethylamino]acridine, Sigma-Aldrich). Aliquots were removed at 20, 45, and 60 min, applied to the sample chambers of a cytospin apparatus (Thermo Shandon), and centrifuged at 850 rpm for 3 min. Dried samples were fixed with cyanoacrylate and slides were examined by epi-illumination UV microscopy on a Zeiss Axioskop (Carl Zeiss). Photographs were made at 630× magnification.

Adherence assay

Sterile coverslips (12 mm diameter, Sigma-Aldrich) were washed in endotoxin-free water and prepared by delivering a 10 μl volume containing various dilutions of one of the following stimulants in HBSS without calcium and magnesium: CCL3 (MIP-1α, Peprotech), CCL4, (MIP-1β, Peprotech), CCL5, (RANTES, Peprotech), CXCL12, (SDF-1, Peprotech), α_1PI (Cat.no.A6150, Sigma-Aldrich), α_1PI (A9024, Sigma-Aldrich), α_1 antichymotrypsin (α_1ACT, Calbiochem), antithrombin III (ATIII, Sigma-Aldrich), C1 esterase inhibitor (Calbiochem), methoxysuccinyl-L-Ala-L-Ala-L-Pro-L-Val-chloromethylketone (MAAPVCK; Sigma-Aldrich), N-tosyl-L-phenylalanine chloromethylketone (TPCK, Sigma-Aldrich), a synthetic peptide representative of the thrombin agonist (SFLLRN, Ser-Phe-Leu-Leu-Arg-Asn), or a synthetic peptide representative of the HIV fusion domain solubilized in 10% ethanol (FLGFL, Phe-Leu-Gly-Phe-Leu).

To coverslips prepared with chemoattractants as described above, 10^6 cells in 90 μl HBSS were mixed to uniformity, and incubated for 30 min in humidified 5% CO_2 at 37°C without dehydration. To detect the interacting effects of stimulants, cells were delivered in an 80 μl volume to coverslips previously prepared with 10 μl of one stimulant, mixed to uniformity, and incubated for 15 min at 37°C. Subsequently, an additional stimulant was delivered in a 10 μl volume to each coverslip, mixed with preincubated cells to uniformity, and incubated for 30–60 min at 37°C. After stringently washing coverslips free of nonadherent cells, adherent cells were fixed by incubation for 10 min at 20°C with 4% paraformaldehyde in PBS containing 2.5 μM of the nuclear staining acridine orange. Slides were examined by epi-illumination UV microscopy on a Zeiss Axioskop Means and SDs were determined by counting adherent cells in at least three fields/coverslip.

Examination of adherence stimulated by various agonists at various time points over a 24 h period suggested optimal effects could be detected between 30 and 60 min. Adherence of clones in independent experiments using identical conditions did not vary. Unstimulated adherence of U937 subclones between independent experiments could be explained in entirety by the bovine serum in which cells had been cultured, suggesting cells were conditioned by unknown serum components as previously demonstrated (2, 3).

Ab array analysis

Cells were cultured, pelleted, extracted, and labeled using the protocol provided with the Ab Microarray 380 kit (BD Clontech). Samples were screened in duplicate using microarray slides preprinted with 509 mAbs. Slides were fluorescently scanned, and data were arranged in the Microarray Analysis Workbook provided. The average internally normalized ratio (INR) was determined to represent the abundance of Ags in clone 17 relative to clone 10. An INR >1 suggests an Ag is more abundant in clone 17 than in clone 10; only INR >1.5 were considered significant. An INR <1 suggests an Ag is more abundant in clone 10; only INR <0.5 were considered significant.

Intracellular phospho-epitope staining for flow cytometry

Cells (1×10^6 cells/well in 96-well plates) were fixed using 1.5% paraformaldehyde in a volume of 100 μl. Cells were washed once with PBS containing 1% BSA (FACS wash) and incubated at 4°C for 10 min in 100 μl ice-cold methanol. Cells were washed twice and incubated at 23°C for 20 min with various phosphoprotein-specific Abs directly conjugated with PE, Alexa Fluor 488, or Alexa Fluor 647 (Molecular Probes). Phosphoproteins measured included Stat1 Tyr-701, Stat3 Tyr-705, Stat4 Tyr-693, Stat5 Tyr-694, Stat6 Tyr-641, NF-κB p65 Ser-529, NF-κB p65 Ser-536, ERK 1/2 Thr-202/Tyr-204, PLC-γ1 Tyr-783, and p38 MAPK Thr-180/Tyr-182, (BD Pharmingen and BD PhosFlow), SLP-76 (provided by BD Pharmingen), Akt Ser-473, Akt Thr-308, JNK, and p53 Ser-15 (Cell Signaling Technologies). Rabbit anti-Akt Thr-308 and mouse anti-p53 Ser-15 were not directly conjugated to fluorochromes, and Ab binding was detected using Alexa Fluor 647 conjugated to anti-rabbit Ig or anti-mouse Ig (Invitrogen Life Technologies), respectively. NF-κB p65

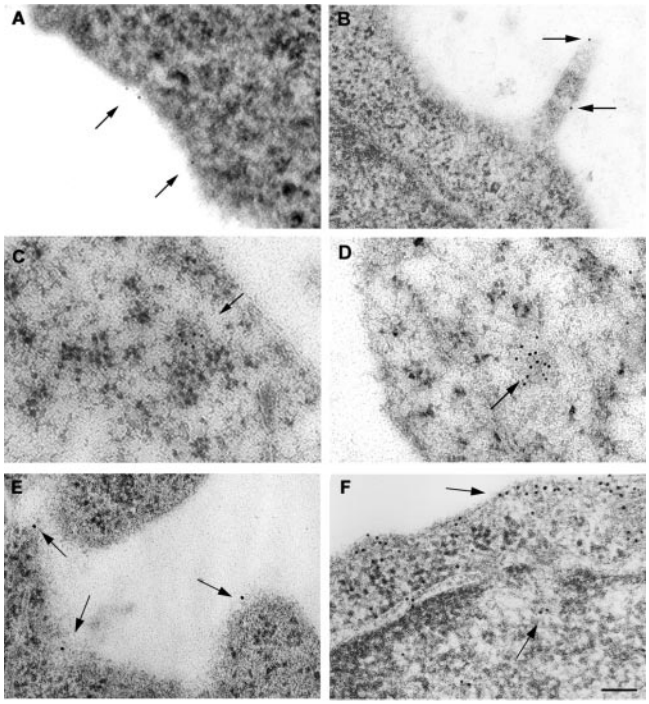

FIGURE 1. Immunolocalization of NF-κB p50, HLE, and CatG. *A–D*, HLE (*A*) and CatG (*B*) were detected only on the cell surface of plus clone 10. HLE (*C*) and CatG (*D*) were detected only in the intracytoplasmic compartment of unstimulated minus clone 17. *E*, HLE, in response to LPS treatment, translocated to the cell surface of minus clone 17. *F*, NF-κB p50 was detected in the nucleus and in proximity to the cytoplasmic membrane of the unstimulated plus clone. Each bar represents 0.1 μm. Cells were prepared for TEM in three separate experiments, examined independently by two investigators, and representative images are presented.

Ser-536 was conjugated to Alexa Fluor 647 using a labeling kit (Invitrogen Life Technologies).

LPS and α_1PI stimulation in serum-free medium

Cells were suspended at 2×10^6 cells/ml in AIM V serum-free medium (Invitrogen Life Technologies) and cultured overnight before use. Complexes between LPS (*E. coli* O26:B6; Sigma-Aldrich) and soluble MD-2 (R&D Systems) in AIM V were stabilized by the addition of sCD14 (R&D Systems) in a mixture containing 10 μg LPS/200 μl/10^6 cells, 0.2 μM MD-2, and 1.0 μM sCD14 in AIM V. Cells were stimulated with α_1PI or with LPS mixture at 37°C, 5% CO_2 for 0, 15, 30, 45, or 60 min in microplates or in microfuge tubes that had been precoated using 10% FBS to prevent adherence.

HIV-1 infectivity

Before the addition of HIV-1 NL4–3 ($TCID_{50} = 10^{5.17}$, Advanced Biotechnologies), 10^6 cells/tube were stimulated with LPS mixture for 60 min in AIM V serum-free medium. Pelleted cells were incubated with 2–5 μl HIV-1 for 2 h at 37°C in a humidified chamber containing 5% CO_2 in the presence or absence of 8 μM T-20 fusion inhibitor (National Institutes of Health AIDS Research and Reference Program) and in the presence or absence of 100 μM α_1PI (Sigma-Aldrich, Cat. no. A9024). Cells were washed free of virus with PBS, resuspended in 2.5 ml AIM V serum-free medium containing the original concentrations of α_1PI, LPS, MD-2, and sCD14 present during infection. Culture supernatants were collected every other day for 10 days and stored at −80°C for analysis of p24 Ag (ZeptoMetrix) or RT activity (ENZCheck; Invitrogen Life Technologies).

Results

Immunolocalization of HLE, CatG, and NF-κB p50

As we have previously demonstrated using TEM, HLE_{CS} localizes to the plasma membrane of plus clone 10 (Fig. 1*A*) (2). In contrast, HLE never localized to the plasma membrane of unstimulated clone 17, but instead was found clustered in structures resembling granules (HLE_G) (Fig. 1*C*). Similarly, we show here that CatG was uniquely associated with the plasma membrane of clone 10 (Fig. 1*B*) and was clustered in granule-like structures in clone 17 (Fig. 1*D*). Both HLE and CatG were found in the nuclei of both clones, and HLE was found specifically associated with nucleoli (data not shown). In addition, CatG was found in rough ER (data not shown). NF-κB p50 was distributed throughout the cytoplasm and nucleus of both clones. Interestingly, in both clones, NF-κB p50 was concentrated near the cell surface plasma membrane on the cytoplasmic side and associated with mitochondria (data not shown) as we have previously demonstrated (13).

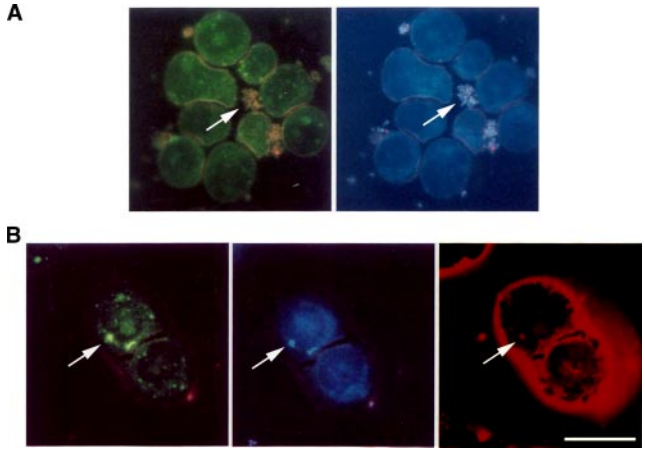

FIGURE 2. Phagocytosis and killing of opsonized bacteria. *A*, Live, opsonized bacteria were detected only exterior to plus clone 10 and were not phagocytosed. Granules and internalized bacteria are visualized using acridine orange (*green*), live bacteria using DAPI (*blue*), and dead bacteria using PI (*red*). *B*, Opsonized bacteria were phagocytosed and killed by minus clone 17. Bacteria can be seen both inside (*green*) and outside the cell (*blue*). One phagosome designated by arrow contains dead bacteria (*red*). Cells and bacteria were examined by two investigators independently in more than three separate experiments, and representative images are presented. Bar represents 20 μm.

Phagocytosis and killing of opsonized bacteria

To determine whether HLE_{CS} exhibits microbicidal activity as HLE_G does, U937 subclones were examined for bacterial uptake and killing. Opsonized *P. gingivalis* was labeled with DAPI and incubated with cells in the presence of acridine orange and PI. Slides were prepared and examined by fluorescence microscopy (Fig. 2) for the presence of live bacteria (blue), dead bacteria or cells (PI), and viable cells (green). For plus clone 10, only live bacteria were detected and were found on the cell exterior, never internalized, indicating this clone is not capable of phagocytosis (Fig. 2*A*). Granules were not detected in these cells by acridine orange, a result consistent with the lack of granules detected by TEM.

In contrast, images of the minus clone 17 revealed clusters of intracellular bacteria, some of which were dead. Granules were visible by acridine orange, confirming their presence as detected by TEM. The presence of killed bacteria is evidence that the minus clone has the capacity to produce an oxidative burst, and is thus competent for phagocytosis and lysosomal fusion.

Adherence stimulated by chemokines and serine proteinase inhibitors

Because cellular adherence is Ca^{2+} independent and is the initiating event in cell motility, receptor responsiveness to various chemoattractants was examined by adherence of clones 10 and 17 to glass coverslips. Cells were harvested from tissue culture and washed free of serum using HBSS. As expected, adherence occurred in the presence or absence of Ca^{2+} and Mg^{2+} (data not shown). Chemotaxis occurs as a kinetically defined sequence of adherence and release. Because adherence was measured in the absence of Ca^{2+} and Mg^{2+}, the absence of adherence in response to an agonist under these conditions may be interpreted to result from the absence of participation of the cognate receptor as an initiating event in cell motility.

Both the plus and minus clones have been shown to be chemotactic in response to CXCL12, although the responses differ in intensity and optimal concentration (14). The plus clone was found in this study not to be adherent in response to any chemokines examined including CXCL12 (Fig. 3 *A*). In contrast, adherence of the plus clone was found to be stimulated by α_1PI with an optimal concentration of 1.25 nM/1 $\times$ 10^5 cells (Fig. 3, *A* and *C*) and by C1 esterase inhibitor (data not shown) with optimal concentration 0.1 nM/1 $\times$ 10^5 cells. Neither antithrombin III (ATIII) nor the CatG inhibitor α_1ACT stimulated adherence of the plus clone (Fig. 3*A*).

Adherence of the minus clone 17 was found to be stimulated by CXCL12, minimally by CCL4, but not by other chemokines (Fig. 3*A*). The optimal concentration for CXCL12 was 12.5 nM/1 $\times$ 10^5 cells. The minus clone was adherent in response to ATIII with an optimal concentration of 0.01 nM/1 $\times$ 10^5 cells, but no response was noted with α_1PI, α_1ACT (Fig. 3*A*), or C1 esterase inhibitor (data not shown). Differences in CXCL12 sensitivity/affinity/reactivity cannot be the result of receptor level, as the U937 plus and minus clones constitutively express sufficient levels of the CXCL12 receptor CXCR4 (100%, MFI 60 and 142, respectively) and CD4 (80%, MFI 215 and 248, respectively) (1, 2). In earlier reports, HLE facilitated detachment of adherent neutrophils (15) and HLE inhibitors suppressed neutrophil chemotaxis (16). We examined adherence of U937 subclones in the presence of a panel of HLE ligands (Fig. 3*B*). The synthetic inhibitor MAAPVCK with specificity for HLE-like proteinases stimulated adherence of the plus clone with an optimal concentration of 100 nM/1 $\times$ 10^5 cells. In contrast, the synthetic inhibitor TPCK with specificity for chymotrypsin-like proteinases stimulated adherence of the plus clone, but exhibited a dose response lacking in optima. These results are consistent with the promiscuous proteinase interactions of TPCK. The minus clone was not adherent in response to either MAAPVCK or TPCK, and these results are consistent with the absence of detectable HLE_{CS}, CatG, or other cell surface granule proteins recognizing these ligands.

Interestingly, the plus clone was found to be adherent in response to the HIV fusion peptide FLGFL (solubilized in 10% ethanol) with an optimal concentration of 1 μM/1 $\times$ 10^5 cells, but not in response to a similar thrombin agonist peptide, SFLLRN. Control studies established that adherence of cells was not influenced by 10% ethanol. The minus clone was not adherent in response to either FLGFL or SFLLRN.

Two known α_1PI receptors expressed on U937 cells are HLE and the well-characterized scavenger receptor, α_2M receptor/low density lipoprotein receptor-related protein (LRP) (17). LRP has been shown to be involved in the binding and uptake of proteinase-complexed proteinase inhibitors including HLE-complexed α_1PI, CatG-complexed α_1ACT, thrombin-complexed ATIII, and C1s-complexed C1 esterase inhibitor. Both the proteinase and inhibitor are inactivated by complexation, and it is the inactivated proteinase inhibitor that binds LRP. Each purified preparation of proteinase or

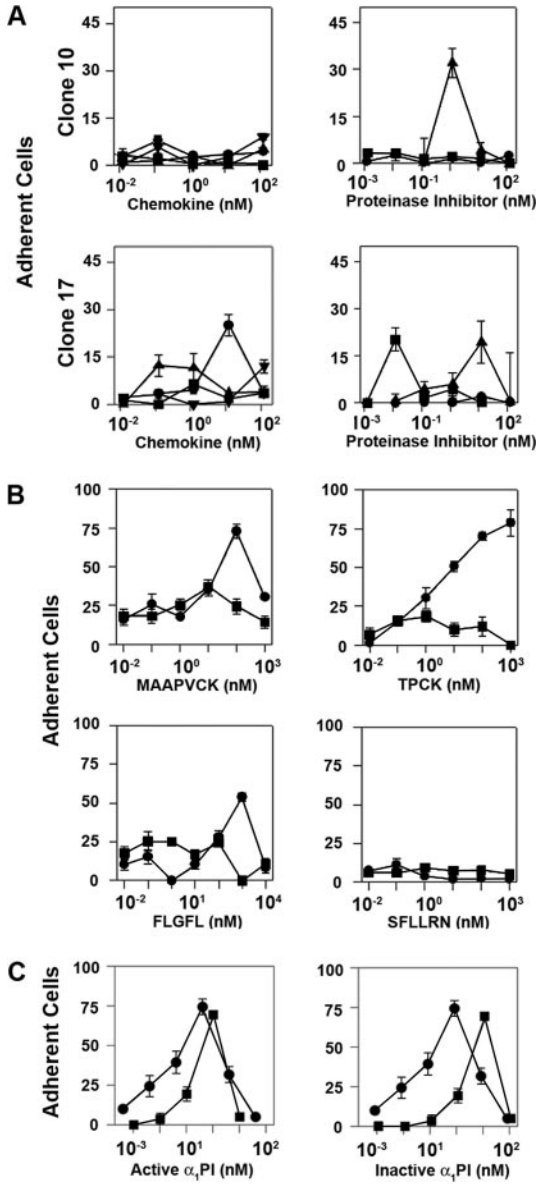

FIGURE 3. Adherence to glass in response to chemokines and serine proteinase inhibitors. *A*, Adherent cells were enumerated in response to chemokines CXCL12α (●), CCL3 (■), CCL4 (▲), and CCL5 (▼) or in response to proteinase inhibitors α_1PI (▲), ATIII (■), and α_1ACT (●). Values represent the mean difference between stimulated and unstimulated adherence. Bars represent SDs. *B*, Plus clone 10 (●), but not minus clone 17 (■), was stimulated to adhere by MAAPVCK, a synthetic peptide inhibitor for HLE and by TPCK, a synthetic peptide inhibitor for chymotrypsin. Plus clone 10 (●), but not minus clone 17 (■), was stimulated to adhere in response to the HIV fusion peptide (FLGFL). The HIV fusion peptide FLGFL was solubilized in 10% ethanol, and unstimulated adherence of cells incubated with 10% ethanol in the absence of peptide was 36 $\pm$ 6 cells/field. Neither subclone was influenced by the thrombin agonist peptide (SFLLRN). Two different preparations of α_1PI were determined to be 32.7% (●) and 8.3% active (■). *C*, Plus clone 10 stimulated by these two α_1PI preparations responded to equivalent optimal concentrations of active α_1PI, but different concentrations of inactive α_1PI. Adherence was optimized for each chemoattractant and adherence induced by each chemoattractant was enumerated in more than three separate experiments.

Table I. *Antigen abundance detected by antibody microarray*[a]

Antigen	Functions	Clone 10	Clone 17
DNA fragmentation factor 45 (DFF45)	Apoptosis; DNA fragmentation		
PEX19	Negative regulation of p53 tumor suppressor factor; peroxisome interactions	√	
RAG-2	Rearrangement of TcR and immunoglobulin genes	√	
Ezrin	Actin anchor to plasma membrane; Cell adhesion; EGFR and TcR tyrosine kinase substrate; Stabilization of the immunologic synapse	√	
MRE11	DNA recombination and repair	√	
Farnesoid X Receptor 2 (FXR2)	Nuclear receptor in cholesterol homeostasis	√	
LEDGF	Expression of heat shock proteins; Strand transfer cofactor of HIV-1 integrase	√	
Neurexin1	Neuron synapse formation and signaling	√	
ECNOS/NOS type III	Anti-apoptotic; Structural component of caveolae; Inhibition of leukocyte adhesion	√	
Glutathione-s-transferase	Oxidative burst		√

[a] Of 509 signaling proteins probed by antibody array, only these 10 proteins were detected to be of significant relative abundance and confirmed by Western blot analysis.

proteinase inhibitor is composed of a unique ratio of active and inactive protein. To discriminate the adherence-inducing α_1PI receptor HLE_{CS}, which recognizes the active form of α_1PI and LRP, which recognizes the inactive form, adherence of U937 subclones was compared using two preparations of active-site standardized α_1PI which were 32.7% and 8.3% active. When the plus clone was stimulated in parallel by these two preparations, adherence was determined to be optimal at equivalent concentrations of active α_1PI (0.3 nM and 0.8 nM/1 $\times$ 10^5 cells), but at 13-fold different concentrations of inactive α_1PI (0.7 nM or 9.3 nM/1 $\times$ 10^5 cells) (Fig. 3*C*). Because of their clonality, all cells should express equal receptor numbers. Thus, we can conclude that it is the active fraction, not the inactive fraction of α_1PI, that is recognized by the adherence-inducing receptor on the plus clone, and further, that the responsible receptor is HLE_{CS}. In support of this result, the minus clone, which does not express HLE on the cell surface, was not adherent to either the active or inactive fraction of α_1PI (data not shown).

Ab array and phospho-epitope analysis

Despite relatively similar cell surface expression of chemotactic receptors, the differences observed between the minus and plus clones in response to various chemoattractants suggested differences in downstream signaling cascades. To investigate signaling profiles, total cytosolic and membrane-associated proteins were extracted from plus clone 10 and minus clone 17 and screened for relative abundance using Ab microarray technology. Those cellular proteins, which were found in comparatively different abundance, were further analyzed by Western blot to confirm identity (data not shown). Several proteins necessary for chemotaxis, immune synapse formation, and resistance to apoptosis were more abundant in the plus clone than in the minus clone (Table I), and this is consistent with the capacity for receptor clustering and capping on the plus clone (2). In contrast, glutathione s-transferase was more abundant in the minus clone reflecting its capacity to generate an oxidative burst as occurs during phagocytic bacterial killing (18).

Comparison of phosphorylation profiles by Western blot analysis (Table II) and by flow cytometry of intracellular phosphoepitopes (Fig. 4) demonstrated that a greater number of biological signatures of the PI3K pathway were phosphorylated in the plus clone than in the minus clone. The minus clone expressed the same pattern of the PI3K signaling components with the exception of Akt phosphorylated at Ser-473 which was not detected by either Western blot or flow cytometry (Fig. 4*A*).

Both nonphosphorylated and phosphorylated p53 tumor suppressor (residues Ser-9, Ser-15, and Ser-20) were detected in the plus clone. Neither the Ser-6 nor Ser-392 phosphorylation forms of p53 were detected in the plus clone. Whereas p53 Ser-15 was phosphorylated in the plus clone, it was not phosphorylated in the minus clone as seen by Western blot analysis, and further confirmed by flow cytometry of intracellular phosphoepitopes (Fig. 4*A*).

Western blot analysis showed that the plus clone expressed phosphorylated forms of SMAD2, STAT3, and cdc2 (data not shown), although phosphorylation of STAT3 could not be confirmed by flow cytometry (data not shown). Not detected by Western blot or flow cytometry in the plus clone were STAT1, STAT4,

Table II. *Phosphorylated antigens detected by Western blot*

Antigen	Functions	Clone 10	Clone 17
PI3K C2β, Akt, p42/p44 MAPK, p38 MAPK, PTEN, PDK1, and GSK3b	EGFR and TcR synapse; Stabilization of HLE/CatG- induced platelet aggregation; Thrombin induced mast cell adhesion; Cell motility	√	√
SMAD2 Ser 463/465	TGFβ signaling pathways	√	√
Cdc2 Tyr-15	Cell motility	√	√
STAT3	IFN, cytokine, and growth factor receptor signaling	√	√
p53 Ser-15	Cell cycle arrest to allow differentiation; Apoptosis; DNA repair	√	
NF-κB p65 Ser-529	Differentiation and apoptosis	√	
Akt Ser-473	Signaling through EGFR	√	
STAT5 Tyr-694	Hematopoiesis and differentiation; IL-6 expression		√

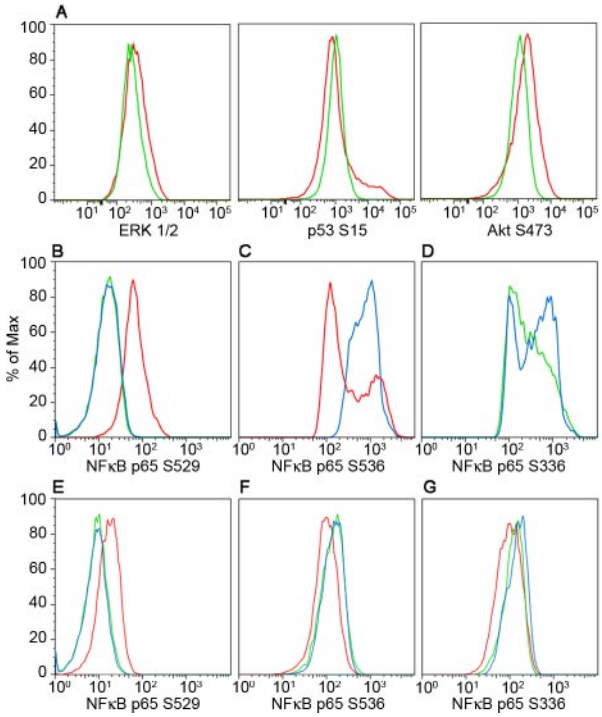

FIGURE 4. Constitutive and induced phosphorylation. *A*, Constitutively phosphorylated ERK 1/2, p53, and Akt Ser-473 were detected in plus clone 10 (*red*), but not minus clone 17 (*green*). *B*, NF-κB p65 Ser-529 was constitutively phosphorylated in plus clone 10 (*red*), but not minus clone 17 (*green*) or LPS-stimulated minus clone (*blue*). *C*, Constitutive NF-κB p65 Ser-536 phosphorylation was at a low level in plus clone 10 (*red*), and was induced by LPS stimulation (*blue*). *D*, Constitutive NF-κB p65 Ser-536 phosphorylation was minimal in minus clone 17 (green) and was induced by LPS stimulation (*blue*). *E*, In plus clone 10, constitutively phosphorylated NF-κB p65 Ser-529 (*red*) was dephosphorylated by incubation with LPS (*green*) or α_1PI (*blue*). In both plus clone 10 (*F*) and minus clone 17 (*G*), phosphorylation of NF-κB p65 Ser-536 was induced by α_1PI (*blue*) as equivalently as by LPS (*green*). Analysis of phospho-epitopes by flow cytometry was performed at least three times by three investigators independently using different instruments and different settings.

STAT5, STAT6, p38, or paxillin. The minus clone expressed phosphorylated forms of SMAD2, STAT3, and STAT5 by Western blot, although phosphorylation of STAT3 or STAT5 could not be confirmed by flow cytometry. Not detected in the minus clone by Western blot or flow cytometry were STAT1, STAT6, and paxillin. Taken together, these results suggest that intact receptor signaling through the PI3K pathway exists in the plus clone in parallel with anti-apoptotic components.

ERK 1/2 was phosphorylated in the plus clone, but not the minus clone (Fig. 4*A*). One of the pathways initiated by ERK phosphorylation is NF-κB activation. Phosphorylated forms of NF-κB p65 and p50 were detected in the plus clone by Western blot (data not shown). Although the minus clone expressed phosphorylated NF-κB p50, almost undetectable levels of phosphorylated p65 were present. Interestingly, the lack of detectable phosphorylated NF-κB p65 was previously suggested to be an artifact of the extraction process whereby p65 was proteolytically cleaved at the carboxyl terminus by HLE_G or CatG in the minus clone, but not the plus clone (10). To address this issue and to circumvent the possibility of extraction-related degradation, intact cells were examined for NF-κB p65 phosphorylation using intracellular phospho-epitope staining for flow cytometry. Examination of intact cells confirmed that NF-κB p65 Ser-529 was phosphorylated in the

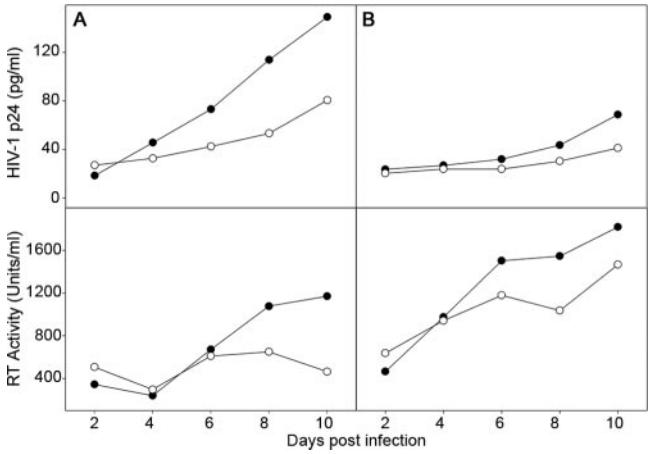

FIGURE 5. RT activity and p24 accumulation by the LPS-stimulated minus clone. Plus clone 10 (*A*) or LPS-stimulated minus clone 17 (*B*) were infected with HIV-1 in serum-free medium containing α_1PI (●), α_1PI, and the T-20 fusion inhibitor (○), or containing no α_1PI (not depicted). Infectivity was performed at least three times, and outcome was determined using p24 Ag capture or RT activity. Representative results are presented.

plus clone, but not the minus clone (Fig. 4*B*). The absence of NF-κB p65 phosphorylation in the minus clone is difficult to reconcile considering that LPS-stimulation of the minus clone is known to confer HIV-1 permissivity (2) and HIV-1 transcription requires phosphorylated NF-κB p65. To further determine whether the clones maintain their ability to phosphorylate NF-κB p65 upon LPS stimulation, cells were stimulated by LPS for various time points and analyzed by phospho-flow. LPS stimulation induced phosphorylation of NF-κB p65 Ser-536 in both plus and minus clones (Fig. 4, *C* and *D*), but did not induce NF-κB p65 Ser-529 in the minus clone. LPS stimulation induced dephosphorylation of NF-κB p65 Ser-529 in the plus clone concurrent with phosphorylation of Ser-536 (Fig. 4*E*). The C-terminal domain of α_1PI, like LPS, stimulates monocytes via CD14 and TLR4 (19). Stimulation of the plus and minus clones by either α_1PI or LPS induced phosphorylation of NF-κB p65 Ser-536 equivalently (Fig. 4, *F* and *G*). Costimulation with LPS and α_1PI at various time points gave no evidence of additive or synergistic effects (data not shown).

HIV-1 infectivity of the LPS-stimulated minus clone

To further characterize the effects of LPS-stimulation on the minus and plus clones, LPS-stimulated cells (as depicted in Fig. 4, *B–D*) were additionally examined for in vitro HIV-1 infectivity. As expected, infectivity of clone 10 was adequately inhibited by the T-20 fusion inhibitor (Fig. 5*A*). Furthermore, LPS-stimulation conferred HIV-1 permissivity to minus clone 17. As we have previously demonstrated, detection of preintegration HIV-1 infectivity by measuring RT enzymatic activity showed greater viral uptake by the LPS-stimulated minus clone 17 than by an equivalent number of infected plus clone 10 cells, and neither the plus clone nor the minus clone were infected by HIV-1 when α_1PI was omitted from serum-free medium (data not shown and Ref. 2). Interestingly, p24 Ag measurement showed that the minus clone produced considerably less p24 than an equivalent number of infected plus clone 10 cells suggesting virion production by the minus clone was not as efficient as the plus clone.

Discussion

The most dramatic difference we found that distinguishes plus clone 10 from minus clone 17 is the capability of the minus clone

to phagocytose and kill opsonized bacteria, a process involving complement receptors CR1 (CD35) and CR3 (CD11b/CD18, Mac-1, $\alpha_M\beta_2$ integrin) (20). Polarization of the plasma membrane commits molecular processes to specific membrane loci such that cells that are undergoing phagocytosis are incapable of simultaneously migrating, and vice versa. Productive uptake of HIV-1 involves the polarization of chemokine receptors which, so far, have not been shown to be a general feature of phagocytosis (21). Furthermore, uptake of HIV-1 by phagocytosis does not result in productive infection (22). Our results herein suggest that, in addition to proteolytic attack, HIV-1 replication may also be blocked after phagocytic uptake because of inherent differences in cell signaling pathways. Heretofore, no studies have undertaken direct comparisons of the receptor-mediated signaling profile that accompanies cell attachment to phagocytic particles and predicates microbicidal activity vs the profile that accompanies cell attachment to tissue matrix and predicates cell migration.

On one hand, phagocytosis involves progressive adherence and extension of the plasma membrane pseudopods along the particle surface until they fuse at their tips to form a phagosome. The characteristic receptors known to mediate phagocytosis recognize Ig or complement fragments that accumulate on bacterial surfaces. The binding of these receptors to their ligands results in receptor clustering in the phagocytic cup, and this clustered arrangement promotes focal phosphorylation, which subsequently induces the PI3K signaling pathway (20) and counterclockwise propagation of Ca^{2+} waves along the entire internal plasma membrane of the cell (23). Exocytosis of lysosomal vesicles and granules to the phagosome precedes sealing of the phagosomal space (24).

Cell migration, in contrast, results from selective and sequential activation and deactivation of receptors (25), consequent polar segregation of related membrane proteins to the leading edge or trailing uropod, and both clockwise and counterclockwise propagation of Ca^{2+} waves along the internal surface of the plasma membrane, which initiate from different locations within the cell (23). Endocytosis of receptors at the trailing edge and their subsequent exocytosis to the leading edge has been proposed to explain endosome receptor recycling as well as providing for the expansion in membrane surface area necessary for extending the cell forward (26). In contrast, this endocytic/exocytic process occurs randomly in stationary cells (27), suggesting involvement of discrete receptors as opposed to the involvement of cocapped receptors that occurs during directional movement. HIV-1 preferentially binds cocapped receptors and was detected both at the leading and trailing edge of the cell (2), and this evidence suggests HIV-1-uptake may occur during the routine process of cell migration vs uptake by discrete receptors on stationary cells.

Although plus and minus clones express similar numbers of CXCR4 and CD4 receptors, only the minus clone was found to attach to CXCL12-coated coverslips, and only the plus clone was found to have the ability to attach to HIV-1 fusion peptide-coated coverslips. Whereas CXCL12 was shown in this study to stimulate adherence of the minus clone, but not the plus clone, the chemotaxis index stimulated by CXCL12 has been previously found to be substantially greater for the plus clone than for the minus clone (1, 14). This suggests that during chemotaxis of the plus clone, CXCL12 exerts its effect at a step subsequent to initial adherence, and that during chemotaxis of the minus clone, CXCL12 exerts its effect during the initial step of adherence. These results suggest that HIV-1 plus and minus subclones use different activation pathways during the attachment step that initiates chemotaxis.

Two important conclusions can be drawn from these results regarding HIV-1 uptake. First, because CXCR4 participates in cell attachment on one clone and not the other, CXCR4 is performing two independent activities during the process of cell migration, perhaps simply due to dimerization characteristics. Second, despite its expression of CD4 and CXCR4, in its unstimulated state, the minus clone is lacking in a principal plasma membrane arrangement that allows either binding to or direct insertion of the fusion peptide.

Although the current model suggests that HIV-1 entry proceeds via direct insertion of the fusion peptide, direct insertion occurs when the virus is in great excess and is likely not the only mechanism and probably not the primary mechanism of productive HIV-1 uptake. Because the plus clone, but not the minus clone, was adherent to HIV fusion peptide FLGFL, those cell surface molecules (proteins or lipids) that bind the hydrophobic HIV-1 fusion peptide are either absent or expressed differently on the minus clone. Significantly, these results suggest the HIV-1 fusion domain specifically interacts with a component that is absent from the plasma membrane of the minus clone. Further, because the fusion peptide specifically and saturably binds HLE_{CS} (2, 28), HLE_{CS}-mediated entry provides one mechanism for productive HIV-1 uptake. This assertion is corroborated by the presence of HLEcs in the plus clone (whether stimulated or not) and in the minus clone only upon stimulation as well as by evidence that HIV-1 infectivity is facilitated by the active fraction of α_1PI (2) and is inhibited by the inactive fraction of α_1PI (29).

Comparison of plus and minus clone signaling profiles suggests that in addition to differences in receptor localization, HIV-1 related signaling differences also exist. Best known for its activity in tumor suppression and apoptosis, p53 phosphorylated at Ser-15 was expressed only in the plus clone. PEX19, also exclusively expressed in the plus clone, is a negative regulator of p53 activity (30). Specific genes affected by p53, which act as key regulators of hematopoiesis, are CCAAT/enhancer binding protein α (C/EBPα) and PU.1, a member of the Ezb transformation-specific sequence family of transcription factors, which regulate expression of HLE and CXCL12. PU.1 activity regulates cell adhesion and phagocytosis, endocytosis, and myeloid and lymphoid development, a process requiring adhesion to stromal cells mediated by the HLE/CXCL12 axis of cell motility/hematopoiesis (31), and this suggests HLE_{CS} and p53 may coordinate in regulating proliferation, differentiation, and apoptosis.

In the absence of NF-κB activation, LTR transcription of Clade B HIV-1 is severely, if not completely, impaired, and this is true of actively as well as latently infected cells (32). Herein, we show that NF-κB p65 Ser-529 is constitutively phosphorylated in the plus clone, but is not phosphorylated in the minus clone even following LPS stimulation (Fig. 5). In fact, both LPS and α_1PI induced dephosphorylation of Ser-529 in the plus clone. At present, there are 19 known phosphatases that regulate NF-κB activity, and at least one of these, PP2A, is endogenously found in complex with NF-κB p65 where it was found to selectively dephosphorylate Ser-536, as opposed to Ser-276 (33). However, dephosphorylation of Ser-529 was not examined by these authors. Concurrently, both LPS and α_1PI induced phosphorylation of Ser-536 in the plus and minus clones (Fig. 4, *F* and *G*) thereby facilitating p65 translocation to the nucleus in a manner previously determined to be independent of IκBα or NF-κB p50 (34). Both LPS and α_1PI were needed to confer HIV-1 permissivity to the minus clone, and this suggests that each provided an independent component required for HIV-1 uptake. Because the LPS-stimulated minus clone exhibited greater RT activity than the plus clone (2), but less p24 accumulation, we propose that HIV-1 binding, entry, and RT activity may be related to HLE_{CS} localization and signaling events in response to α_1PI-induced receptor cocapping.

In addition to NF-κB nuclear translocation, NF-κB posttranslational modification contributes to regulating target gene expression. It has been determined by others that lack of sufficient phosphorylation of NF-κB p65 Ser-536 results from deficient ERK content in murine epidermal cells which in turn contributes to low levels of IKKβ (35), a finding supported herein using human promonocytic cells. Significantly, these authors demonstrated in an NF-κB transient transfection model that NF-κB transactivational activity was abolished by blocking phosphorylation of p65 Ser-536, but not Ser-529 (35). This structural analysis and the evidence presented herein suggest that productive HIV-1 uptake and p24 production efficiency may be related to NF-κB p65 phosphorylation. In situ manipulation of NF-κB phosphorylation sites during each step of interaction between HIV-1 and its various host cell types are necessary to further define the relationship between HIV-1 expression and NF-κB phosphorylation.

Acknowledgments

We thank Drs. H. Moriuchi and A. S. Fauci for providing U937 subclones and I. Carlo for discussion and advice.

Disclosures

The authors have no financial conflict of interest.

References

1. Moriuchi, H., M. Moriuchi, J. Arthos, J. Hoxie, and A. S. Fauci. 1997. Promonocytic U937 subclones expressing CD4 and CXCR4 are resistant to infection with and cell-to-cell fusion by T-cell-tropic human immunodeficiency virus type 1. *J. Virol.* 71: 9664–9671.
2. Bristow, C. L., D. R. Mercatante, and R. Kole. 2003. HIV-1 preferentially binds receptors co-patched with cell surface elastase. *Blood* 102: 4479–4486.
3. Bristow, C. L., H. Patel, and R. R. Arnold. 2001. Self antigen prognostic for human immunodeficiency virus disease progression. *Clin. Diagn. Lab. Immunol.* 8: 937–942.
4. Bangalore, N., and J. Travis. 1994. Comparison of properties of membrane bound versus soluble forms of human leukocytic elastase and cathepsin G. *Biol. Chem. Hoppe-Seyler* 375: 659–666.
5. Gullberg, U., A. Lindmark, G. Lindgren, A. M. Persson, E. Nilsson, and I. Olsson. 1995. Carboxyl-terminal prodomain-deleted human leukocyte elastase and cathepsin G are efficiently targeted to granules and enzymatically activated in the rat basophilic/mast cell line RBL. *J. Biol. Chem.* 270: 12912–12918.
6. Tavor, S., I. Petit, S. Porozov, P. Goichberg, A. Avigdor, S. Sagiv, A. Nagler, E. Naparstek, and T. Lapidot. 2005. Motility, proliferation, and egress to the circulation of human AML cells are elastase dependent in NOD/SCID chimeric mice. *Blood* 106: 2120–2127.
7. Cepinskas, G., M. Sandig, and P. R. Kvietys. 1999. PAF-induced elastase-dependent neutrophil transendothelial migration is associated with the mobilization of elastase to the neutrophil surface and localization to the migrating front. *J. Cell Sci.* 112: 1937–1945.
8. Valenzuela-Fernandez, A., T. Planchenault, F. Baleux, I. Staropoli, K. Le Barillec, D. Leduc, T. Delaunay, F. Lazarini, J. L. Virelizier, M. Chignard, and F. Arenzana-Seisdedos. 2002. Leukocyte elastase negatively regulates stromal cell-derived factor-1 (SDF-1)/CXCR4 binding and functions by animo-terminal processing of SDF-1 and CXCR4. *J. Biol. Chem.* 277: 15677–15689.
9. Wolf, K., R. Muller, S. Borgmann, E. B. Brocker, and P. Friedl. 2003. Amoeboid shape change and contact guidance: T-lymphocyte crawling through fibrilar collagen is independent of matrix remodeling by MMPs and other proteases. *Blood* 102: 3262–3269.
10. Franzoso, G., P. Biswas, G. Poli, L. M. Carlson, K. D. Brown, M. Tomita-Yamaguchi, A. S. Fauci, and U. K. Siebenlist. 1994. A family of serine proteases expressed exclusively in myelo- monocytic cells specifically processes the nuclear factor-κB subunit p65 in vitro and may impair human immunodeficiency virus replication in these cells. *J. Exp. Med.* 94: 1445–1456.
11. Qian, J., V. Bours, J. Manischewitz, R. Blackburn, U. Siebenlist, and H. Golding. 1994. Chemically selected subclones of the CEM cell line demonstrate resistance to HIV-1 infection resulting from a selective loss of NF-κB DNA binding proteins. *J. Immunol.* 152: 4183–4191.
12. Bristow, C. L., F. di Meo, and R. R. Arnold. 1998. Specific activity of α1proteinase inhibitor and α2macroglobulin in human serum: application to insulin-dependent diabetes mellitus. *Clin. Immunol. Immunopathol.* 89: 247–259.
13. Cogswell, P. C., D. F. Kashatus, J. A. Keifer, D. C. Guttridge, J. Y. Reuther, C. Bristow, S. Roy, D. W. Nicholson, and A. S. Baldwin. 2002. NF-κ B and Iκ Bα are found in the mitochondria: evidence for regulation of mitochondrial gene expression by NF-κB. *J. Biol. Chem.* 278: 2963–2968.
14. Moriuchi, H., M. Moriuchi, and A. S. Fauci. 1998. Differentiation of promonocytic U937 subclones into macrophage-like phenotypes regulates cellular factor(s) which modulate fusion/entry of macrophage-tropic human immunodeficiency virus type 1. *J. Virol.* 72: 3394–3400.
15. Cai, T. Q., and S. D. Wright. 1996. Human leukocyte elastase is an endogenous ligand for the integrin CR3 (CD11b/CD18, Mac-1,$\alpha_M\beta_2$) and modulates polymorphonuclear leukocyte adhesion. *J. Exp. Med.* 184: 1213–1223.
16. Sarfati, I., D. Lopes, E. A. Murphy, S. Rao, and J. R. Cohen. 1996. Inhibition by protease inhibitors of chemotaxis induced by elastin-derived peptides. *J. Surg. Res.* 61: 84–88.
17. Conese, M., A. Nykjaer, C. M. Petersen, O. Cremona, R. Pardi, P. A. Andreason, J. Gliemann, E. I. Christensen, and F. Blasi. 1995. α-2-macroglobulin receptor/Ldl receptor-related protein (Lrp)-dependent internalization of the urokinase receptor. *J. Cell Biol.* 131: 1609–1622.
18. Kirlin, W. G., J. Cai, S. A. Thompson, D. Diaz, T. J. Kavanagh, and D. P. Jones. 1999. Glutathione redox potential in response to differentiation and enzyme inducers. *Free Radical Biol. Med.* 27: 1208–1218.
19. Subramaniyam, D., P. Glader, K. von Wachenfeldt, J. Burneckiene, T. Stevens, and S. Janciauskiene. 2006. C-36 peptide, a degradation product of α1-antitrypsin, modulates human monocyte activation through LPS signaling pathways. *Int. J. Biochem. Cell. Biol.* 38: 563–575.
20. Greenberg, S. 1995. Signal transduction of phagocytosis. *Trends Cell Biol.* 5: 93–99.
21. Phadke, A. P., G. Akangire, S. J. Park, S. A. Lira, and B. Mehrad. 2007. The role of CC chemokine receptor 6 in host defense in a model of invasive pulmonary aspergillosis. *Am. J. Respir. Crit. Care Med.* 175: 1165–1172.
22. Trujillo, J. R., R. Rogers, R. M. Molina, F. Dangond, M. F. McLane, M. Essex, and J. D. Brain. 2007. Noninfectious entry of HIV-1 into peripheral and brain macrophages mediated by the mannose receptor. *Proc. Natl. Acad. Sci. USA* 104: 5097–5102.
23. Kindzelskii, A. L., and H. R. Petty. 2003. Intracellular calcium waves accompany neutrophil polarization, formylmethionylleucylphenylalanine stimulation, and phagocytosis: a high speed microscopy study. *J. Immunol.* 170: 64–72.
24. Tapper, H., W. Furuya, and S. Grinstein. 2002. Localized exocytosis of primary (lysosomal) granules during phagocytosis: role of $Ca2^+$-dependent tyrosine phosphorylation and microtubules. *J. Immunol.* 168: 5287–5296.
25. Wright, S. D., and B. C. Meyer. 1986. Phorbol esters cause sequential activation and deactivation of complement receptors on polymorphonuclear leukocytes. *J. Immunol.* 136: 1759–1764.
26. Thompson, C. R. L., and M. S. Bretscher. 2002. Cell polarity and locomotion, as well as endocytosis, depend on NSF. *Development* 129: 4185–4192.
27. Bretscher, M. S. 1984. Endocytosis: relation to capping and cell locomotion. *Science* 224: 681–686.
28. Bristow, C. L., S. A. Fiscus, P. M. Flood, and R. R. Arnold. 1995. Inhibition of HIV-1 by modification of a host membrane protease. *Int. Immunol.* 7: 239–249.
29. Munch, J., L. Standker, K. Adermann, A. Schulz, M. Schindler, R. Chinnadurai, S. Pohlmann, C. Chaipan, T. Biet, T. Peters, et al. 2007. Discovery and optimization of a natural HIV-1 entry inhibitor targeting the gp41 fusion peptide. *Cell* 129: 263–275.
30. Sugihara, T., S. C. Kaul, J. Y. Kato, R. R. Reddel, H. Nomura, and R. Wadhwa. 2001. Pex19p dampens the p19ARF-p53-p21WAF1 tumor suppressor pathway. *J. Biol. Chem.* 276: 18649–18652.
31. Lapidot, T., and I. Petit. 2002. Current understanding of stem cell mobilization: the roles of chemokines, proteolytic enzymes, adhesion molecules, cytokines, and stromal cells. *Exp. Hematol.* 30: 973–981.
32. Williams, S. A., H. Kwon, L. F. Chen, and W. C. Greene. 2007. Sustained induction of NF-κB is required for efficient expression of latent human immunodeficiency virus type 1. *J. Virol.* 81: 6043–6056.
33. Li, S., L. Wang, M. A. Berman, Y. Zhang, and M. E. Dorf. 2006. RNAi screen in mouse astrocytes identifies phosphatases that regulate NF-κB signaling. *Mol. Cell.* 24: 497–509.
34. Sasaki, C. Y., T. J. Barberi, P. Ghosh, and D. L. Longo. 2005. Phosphorylation of RelA/p65 on serine 536 defines an IκBα-independent NF-κB pathway. *J. Biol. Chem.* 280: 34538–34547.
35. Hu, J., H. Nakano, H. Sakurai, and N. H. Colburn. 2004. Insufficient p65 phosphorylation at S536 specifically contributes to the lack of NF-κB activation and transformation in resistant JB6 cells. *Carcinogenesis* 25: 1991–2003.